Journal of Electronic Materials, Vol. 23, No. 6, 1994

Active Brazing Alloy Paste as a Totally Metal Thick Film Conductor Material

MINGGUANG ZHU and D.D.L. CHUNG

Composite Materials Research Laboratory, Furnas Hall, State University of New York at Buffalo, Buffalo, NY 14260-4400

A silver-based active (titanium-containing) brazing alloy, namely 63Ag-34.25Cu-1.75Ti-1.0Sn, was found to serve as a totally metal (no glass) thick film conductor which exhibited lower electrical resistivity, much greater film/substrate adhesion, much lower porosity, similar solderability, and lower scratch resistance compared to the conventional silver-glass thick film. The brazing alloy film was formed by screen printing a paste containing the alloy particles and then firing at 880°C in vacuum.

Key words: Active brazing alloy, metal thick film conductor

INTRODUCTION

Electrical conductors in the form of thick films applied by screen printing a paste on a substrate are the dominant form of interconnection used in the electronic packaging industry. The thick film conductor is conventionally a metal/glass composite in which the metal serves as the conducting phase and the glass serves as the binder. The thick film conductor is formed by applying a paste (comprising the metal powder, glass frit, and a vehicle) on a substrate by screen printing and then firing to cause the glass to flow and the metal particles to sinter together. Due to the presence of the glass in the thick film, the electrical resistivity is 2–4 times that of the corresponding bulk metal.[1]

As low resistivity is of primary importance, it is desirable to remove the glass from the paste so that the film is totally metal. On the other hand, this removal will require the use of an alternate mechanism for bonding the film to the substrate. It is, thus, the objective of this paper to develop a totally metal thick film that exhibits lower resistivity than conventional silver-based thick film conductor and yet exhibits at least as strong a film-substrate bond strength as conventional thick film. Moreover, the total metal thick film must be screen printable. This objective was reached by the use of an active brazing alloy paste as the thick film paste. This alloy contains titanium as a minor alloying element,[2,3] which reacts with the ceramic substrate, thus causing bonding between the alloy and the ceramic substrate. The silver-based active brazing alloy thick film was found to exhibit a lower resistivity than the conventional silver-based thick film and exhibited an even stronger film-substrate bond strength than the conventional thick film. This paper provides a detailed comparison of the two kinds of thick films in terms of the electrical resistivity, solderability, film-substrate adhesion, scratch resistance, and the patternability.

(Received November 12, 1993; revised February 9, 1994)

EXPERIMENTAL

Materials

Pastes

Two kinds of pastes were used for thick film preparation. The first kind (referred to as A) is a commercial thick film paste, namely the 6160 silver conductor

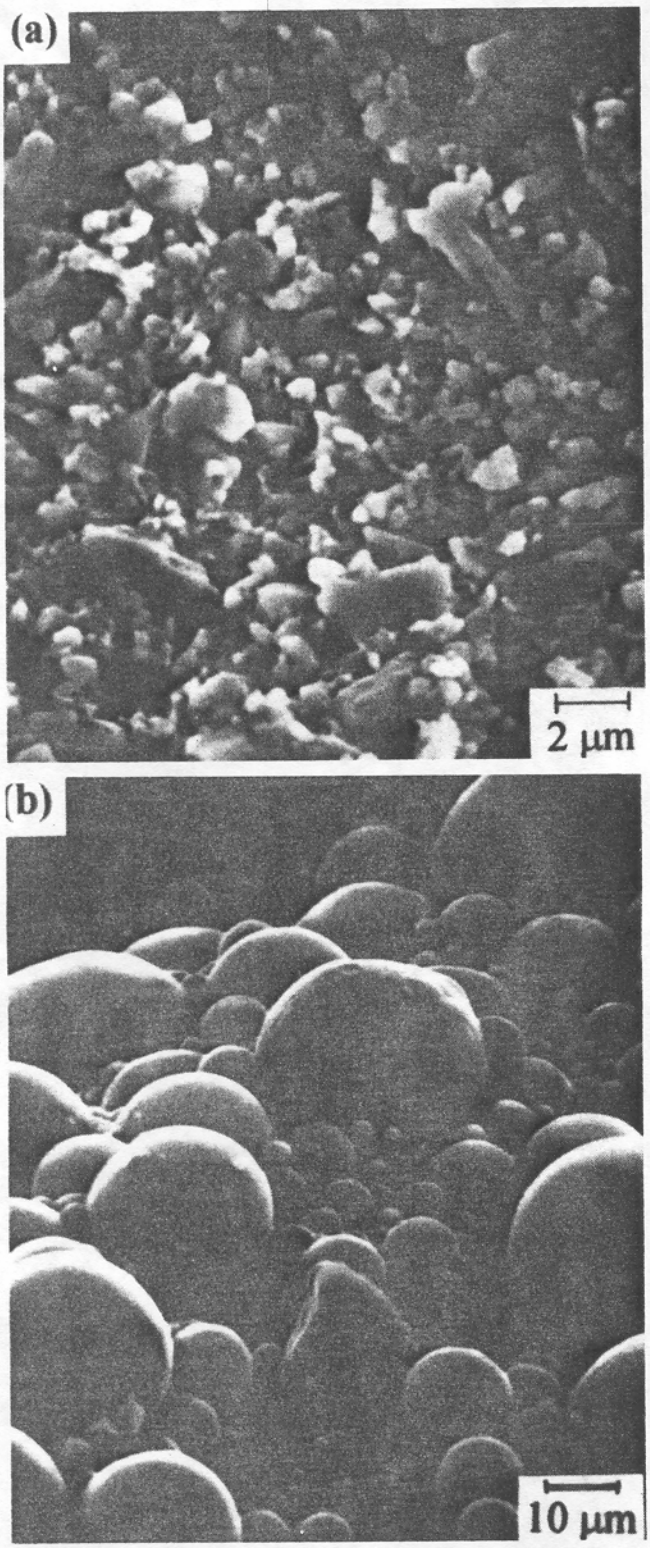

Fig. 1. Scanning electron microscopy photographs of (a) the A paste, and (b) the B paste.

thick film paste from DuPont Electronics, Manati, Puerto Rico; it was comprised of silver particles, glass frit, and a vehicle. The average particle size was around 1 μm (Fig. 1a). The second kind (referred to as B) is an active brazing paste, namely Cusin-1 ABA from WESGO, Belment, California; it contained no glass; the chemical composition was 63% Ag + 34.25%Cu + 1.75%Ti + 1.0%Sn (by weight); most of the particles were around 15~20 μm in size (Fig. 1b).

Substrate

The standard 25.4 × 25.4 × 1.6 mm alumina substrate for the thick film industry was used. It contained 96% wt. Al_2O_3 and was made by the 3M Corporation.

Printing

The printing machine used was a PRESCO Screen Printer, Model 432, made by Affiliated Manufacturers, Inc., New Jersey. Stainless steel screens of mesh size #325 were used; they bore printed patterns provided by DuPont Electronics.

Firing

Two firing processes were used. The firing procedure for the A film was 150°C in air for 2 min, followed by 850°C in air for 20 min. The B film was fired in vacuum (~10^{-5} Torr) at 880°C for 10 min.

Adhesion Test

The film/substrate adhesion was tested by peeling and upon pulling in a direction perpendicular to the interface. The objective was to measure the film/substrate debonding strength.

Peel Test

The standard peel test method[4] was used. Crooks were carefully shaped at one end of each copper wire (0.81 mm diam), as shown Figs. 2a–2c. Then, the wires were slipped onto a test pattern with the wire centered over the test pads (2 × 2 mm square). Each lead grips the substrate edge immovably at its crooked end, such that it is in contact with the underlying pads.

Specimens were degreased by acetone and then a layer of flux was applied on the surface of the film. A molten solder bath (63Sn-37Pb) was held at 230°C, and its surface was free of flux residues and dross. A substrate was vertically dipped into the solder bath, such that about two-thirds of the substrate was immersed. Thus, only some of the adhesion test pads were immersed, as illustrated in Figs. 2d and 2e. The dwell time was 5 s. Soldered specimens were cleaned in acetone. The wires were then bent, as shown in Fig. 2d. The peel tests were conducted using a Sintech 2/D materials testing system operated at a crosshead speed of 0.1 mm/min. The peak load was recorded as the break load.

Pull Test

For the A film, a copper wire (1.2 mm diam) was soldered perpendicular to the printed thick film pattern (2 × 2 mm), as shown in Fig. 3a. For the B film, a stainless steel bar (3.1 mm diam) was attached perpendicular to the just printed film (Fig. 3b) and the combination was then fired together in vacuum.

Pulling was in the direction perpendicular to the

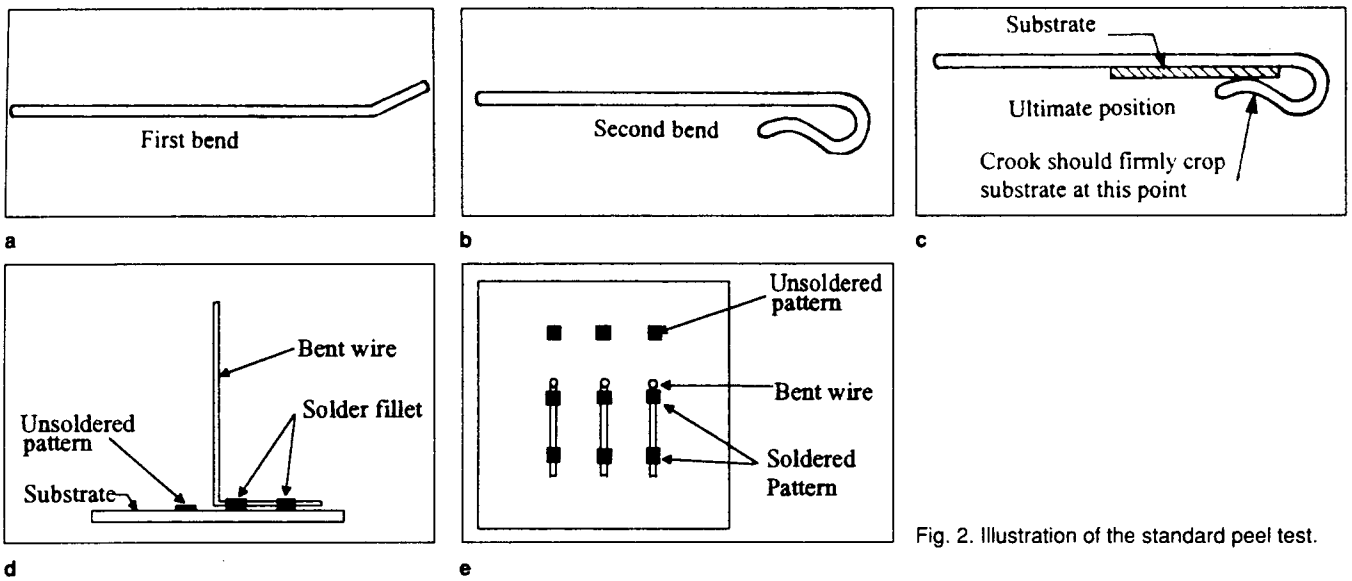

Fig. 2. Illustration of the standard peel test.

film surface. The pull strength was measured by the Sintech 2/D materials testing system operated at a crosshead speed of 0.1 mm/min.

Electrical Resistivity Test

The four-probe method was used to measure the volume electrical resistivity of each film. The four contacts were soldered on.

Solderability Test

An ASTM standard method[5] was used to determine the solderability of the thick films. The fired thick films were covered with a layer of rosin soldering flux. Solder balls (63Sn-37Pb, 0.46 ± 0.03 mm in diam) were then applied to the thick film surface. After placing the substrate with the solder balls on a hot plate at 230°C for 30 s, the specimen was removed and placed on a chill block at room temperature. A scaled optical microscope lens was used to measure the diameter of the solder ball. The larger the diameter of the solder ball after the liquid solder spreading at 230°C, the greater is the solderability.

Scratch test

A 502 shear/scratch tester, made by Teledyne Taber of North Tonawanda, New York, was used to perform the scratch test[6] for the purpose of testing the scratch resistance of the thick films. The specimen was mounted on a horizontally rotatable plate. The scratching tool was attached to a finely balanced scale beam calibrated in grams. A tungsten carbide (WC) scratching tool was used. It had a cutting edge in the form of a corner of a cube; i.e., with three edges of the cube coming together at the corner. The load used was 500 g. After the loaded beam with the scratching tool had come in contact with the thick film surface, the plate which held the specimen was slowly rotated until the tool had moved to the edge of the specimen. Afterward, the resulting scratch was examined under a scanning electron microscope.

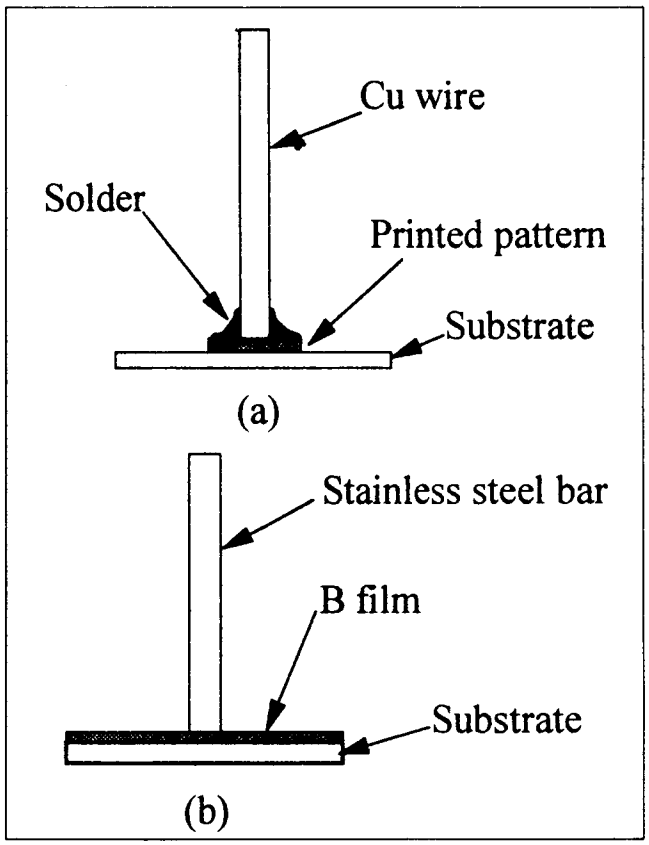

Fig. 3. Sample configuration for the pull test for (a) the A film, and (b) the B film.

RESULTS

Adhesion Test

Peel Test

The results for the peel test are shown in Table I. For the A film, debonding occurred between the film and the substrate. For the B film, debonding occurred between the copper wire and the solder, such that the film/substrate bond never failed during the peel test.

Table I. Results of the Peel Test

A	2.0 ± 0.41 Kg
B	2.7 ± 0.26 Kg

Note: Samples tested: 12 of each type.

Table II. Results of the Pull Test

A	8.8 ± 1.2 MPa
B	21.9 ± 0.6 MPa

Note: Samples tested: 9 of each type.

Table III. Results of the Electrical Resistivity Test

A	$9.57 \times 10^{-6} \pm 0.10 \times 10^{-6}$ Ω.cm
B	$2.34 \times 10^{-6} \pm 0.16 \times 10^{-6}$ Ω.cm

Note: Samples tested: 9 of each type.

Table IV. Results of the Solderability Test

	Solder Ball Diameter (mm)	
	Before Melting	After Melting
A	0.46 ± 0.03	9.95 ± 0.10
B	0.46 ± 0.03	0.96 ± 0.18

Note: Samples tested: 22 of each type.

Thus, only a lower bound of the film/substrate debonding load was measured for the B film case. Nevertheless, the high value of this lower bound indicates a stronger film/substrate bond in the B case compared to the A case.

Pull Test

Table II shows the result of the pull test. For the A film, the debonding occurred between the film and the substrate. For the B film, the failure occurred inside the substrate; thus, only a lower bound of the film/substrate debonding strength was measured in the B case. The very high value of this lower bound indicates that the film/substrate bond is much stronger in the B case than in the A case.

Electrical Resistivity

Table III shows the results of the electrical resistivity test. The resistivity was lower for B than A.

Solderability

Table IV shows the results of the solderability test. The solderability was similar for A and B.

Scratch Test

The scratch test shows that the depth and width of the scratches were similar for the two kinds of films. For the A film, the scratch edges were smooth, showing that the Ag-glass material exhibited brittle behavior during scratching. For the B film, the scratch edges were not smooth; some flakes came off from B during scratching and were observed to protrude from the scratch edges. Thus, B was not as scratch resistant as A.

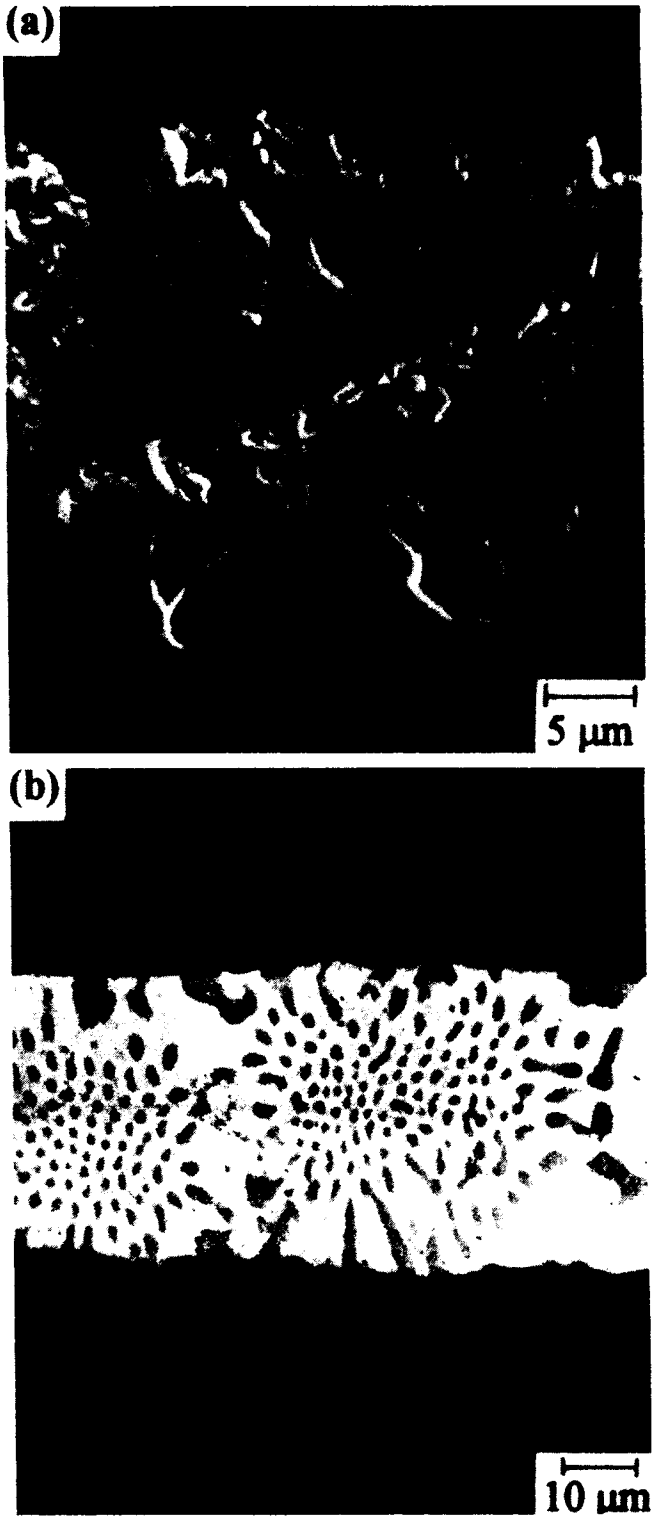

Fig. 4. Two SEM photographs of the cross sections of (a) the A film, and (b) the B film. The bottom of each film is the Al_2O_3 substrate.

CORRELATION WITH THE MICROSTRUCTURE

Scanning electron microscopy (SEM), together with

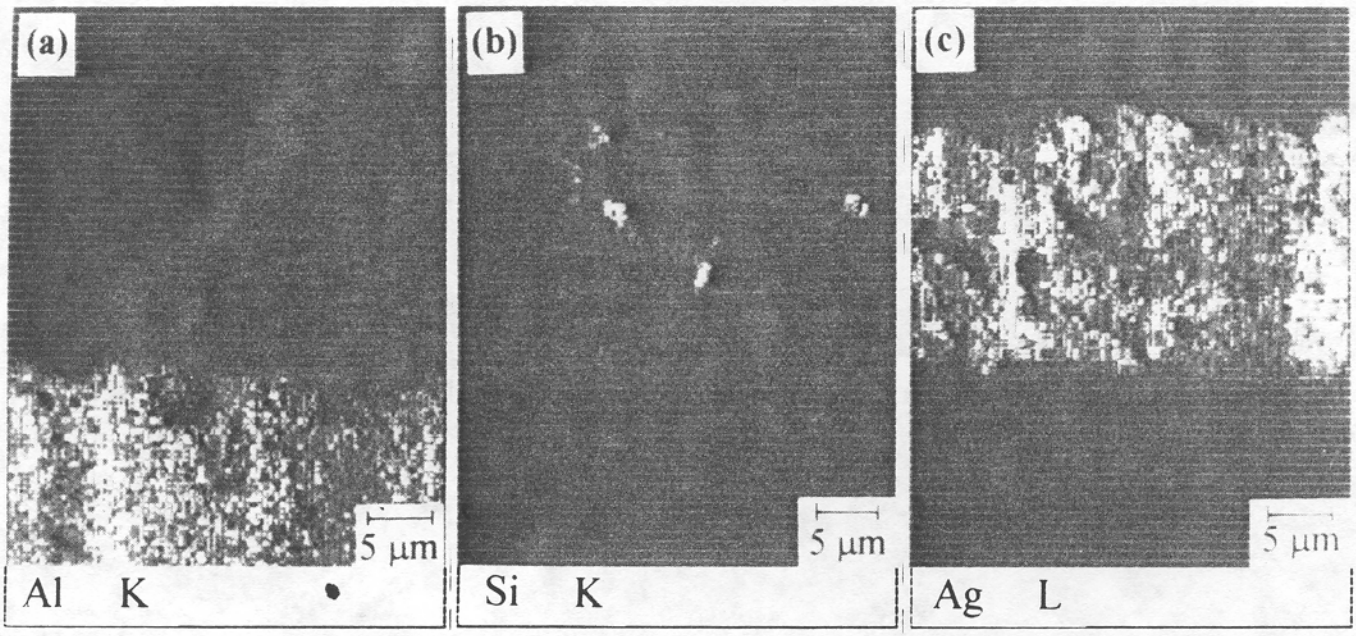

Fig. 5. Elemental x-ray maps of the cross section of the A film shown in Fig. 4a.

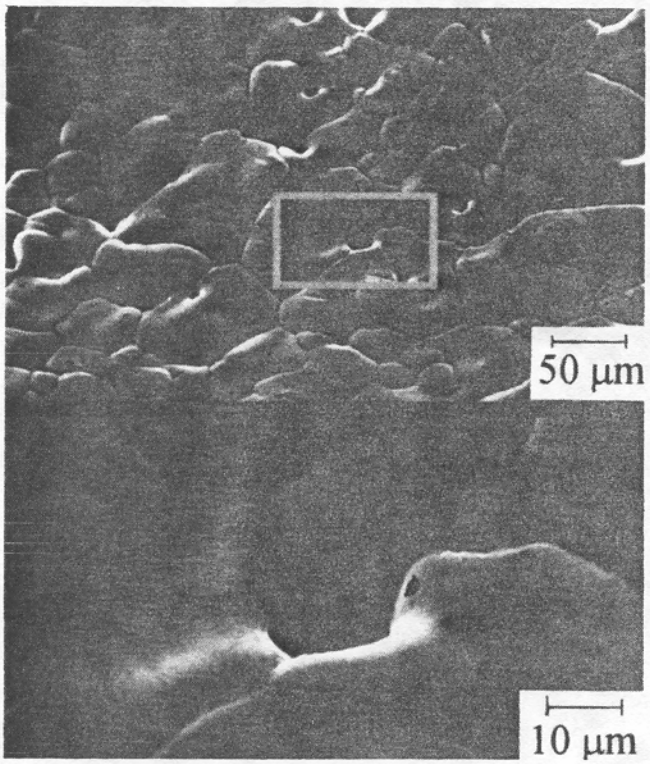

Fig. 6. Scanning electron microscopy photographs at two magnifications of the top of the A film.

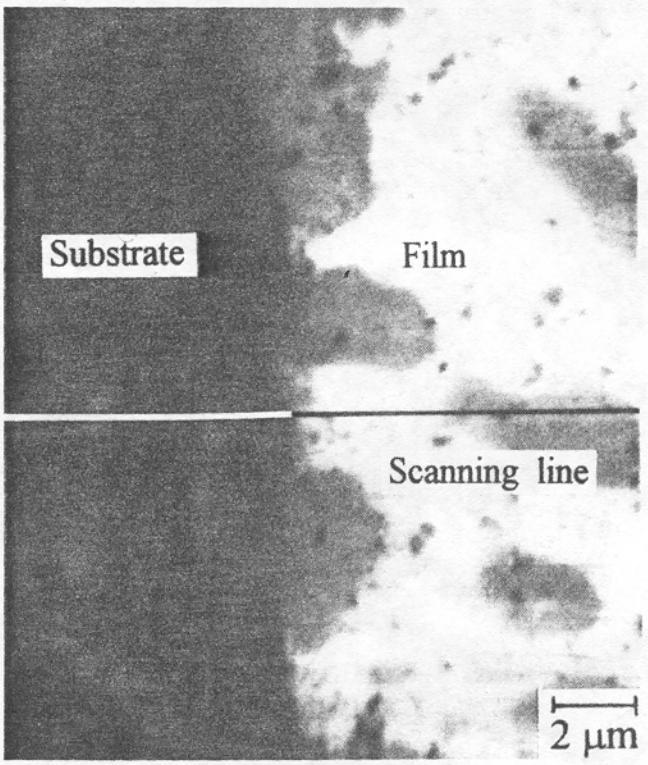

Fig. 7. Scanning electron microscopy photograph showing the film/substrate interface for the B film.

the associated electron probe microanalysis and elemental x-ray mapping, were used to study the film/substrate interface and the film microstructure. The purpose is to explain the above results from the microstructure.

Within Fig. 4 are the SEM photographs of the cross sections of the two kinds of thick films. The A film (Fig. 4a), 20 μm thick, contained a lot of pores, whereas the B film, 40 μm thick, exhibited no porosity.

Figure 5 shows the elemental x-ray maps of the cross section of the A film shown in Fig. 4a. The Si x-ray map shows the presence of a glass phase both inside the film and at the surface of the film.

Figure 6 shows the top view of the A film. Pores were present both at the grain boundaries and within the grains.

Figure 7 shows the interface structure of the film/substrate interface for the B film. No gap was ob-

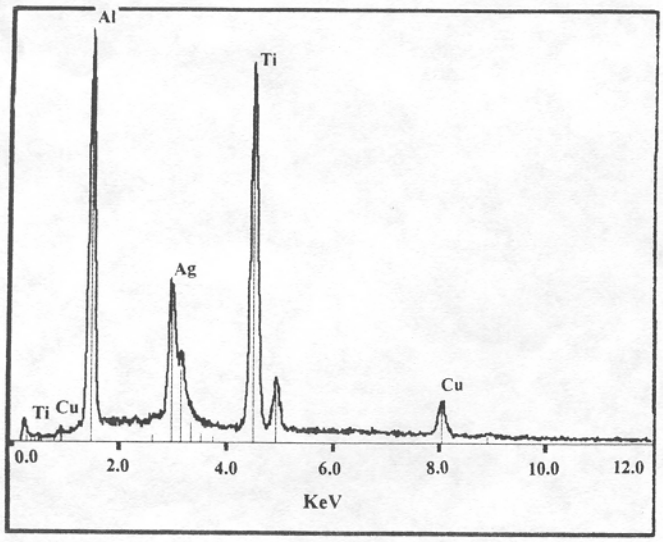

Fig. 8. X-ray spectrum at a point at the film/substrate interface for the B film.

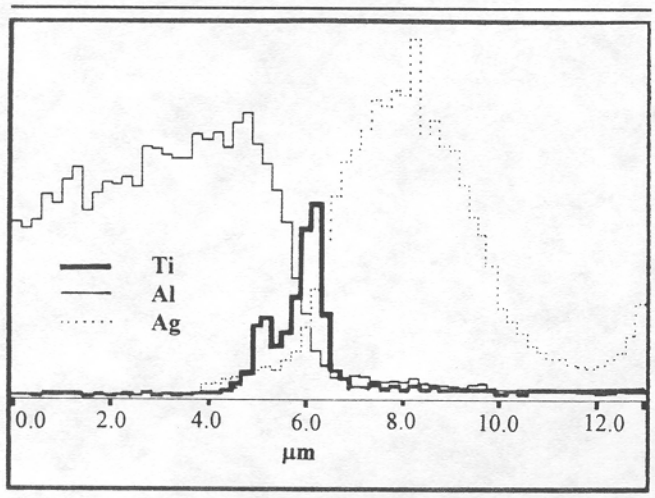

Fig. 9. Variation of the heights of the x-ray peaks associated with various elements (Ti, Al, and Ag) along a line across the film/substrate interface for the B film.

served at the interface, indicating good bonding. The x-ray spectrum at a point at the interface (Fig. 8) and its variation along a line across the interface (Fig. 9) show titanium segregation (a titanium-rich reaction product layer) at the interface, due to the reaction between titanium in the film and the substrate. This reaction helped the bonding between the film and the substrate, as is well-known in the field of active brazing alloys.

Figures 10a and 10b show the printed pattern (before firing) of A and B, respectively. The patternability was worse for B than A. Figures 11a and 11b show at a higher magnification the top view of the edge of a printed line from each of the two panels of Fig. 10. These photographs show that the particle size in the paste was much larger for B than for A. This particle size difference caused the difference in patternability.

Figures 12a and 12b show the cross-sectional view of the A and B films, respectively, before firing. The particles of the B paste were so large that even one

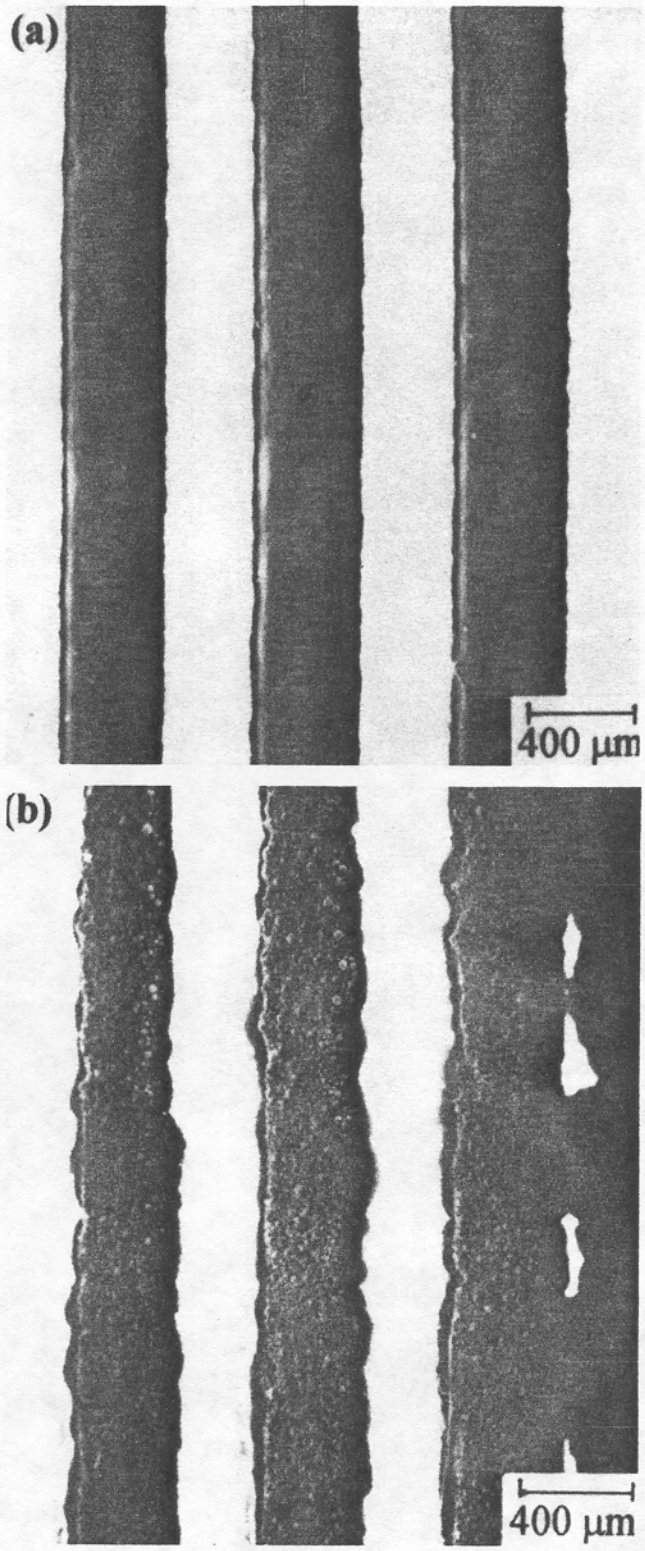

Fig. 10. Scanning electron microscopy photographs of the printed film pattern before firing of (a) the A film, and (b) the B film.

particle could occupy the whole thickness of the film.

Figures 13a and 13b show the cross-sectional view of the A and B films, respectively, after firing. The films looked similar after firing (Fig. 13), although they looked different before firing (Fig. 12).

Figures 14a and 14b show the top view of two films after firing. The surface of both films was smooth. However, the edge of the B film (Fig. 14b) was not as sharp as that of the A film, though the difference was small. In contrast, the difference was large before firing.

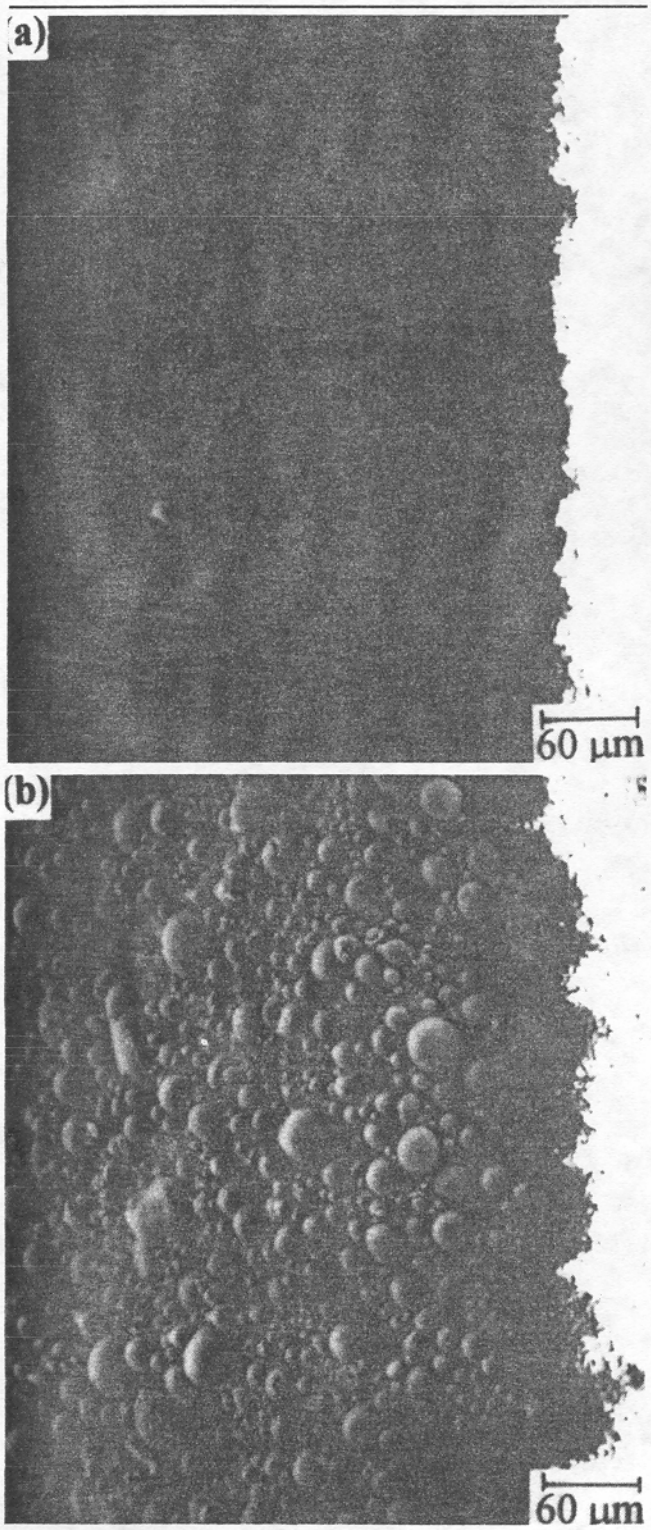

Fig. 11. Scanning electron microscopy photographs of the top view of the edge of a printed conductor line before firing for (a) the A film, and (b) the B film.

DISCUSSION

The comparison between the A and B films is summarized in Table V. The B film is superior to the A film in its lower electrical resistivity, much greater film/substrate adhesion and much lower porosity.

The high porosity and the existence of the glass phase in the A film are the main reasons for the high resistivity of the A film compared to the B film, which is a totally metal layer, as shown in Fig. 4b.

As shown in Fig. 8 and Fig. 9, the Ti in the B paste was concentrated at the film/substrate interface, indicating that there was a reaction layer at the interface. It was this reaction layer that constituted the film-substrate bond and provided the high film-sub-

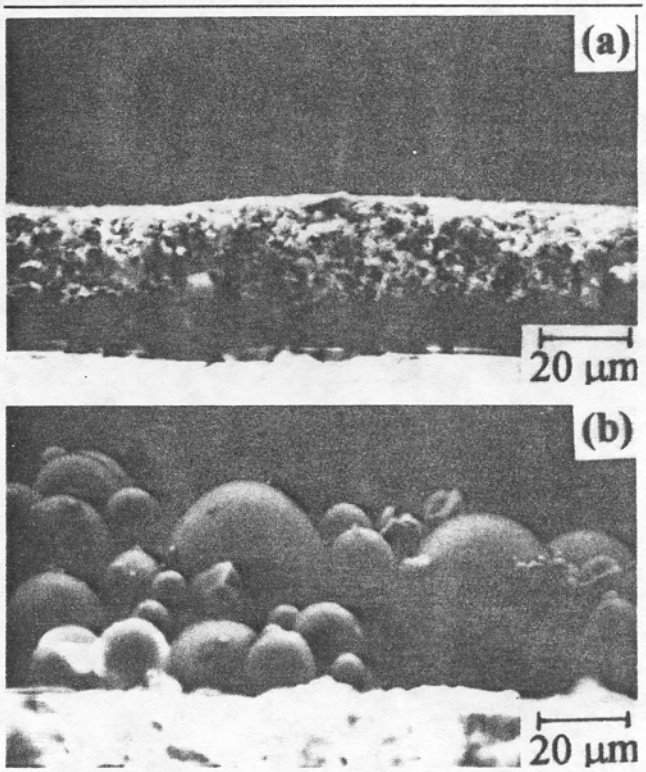

Fig. 12. Scanning electron microscopy photographs of the cross-sectional view before firing of (a) the A film, and (b) the B film.

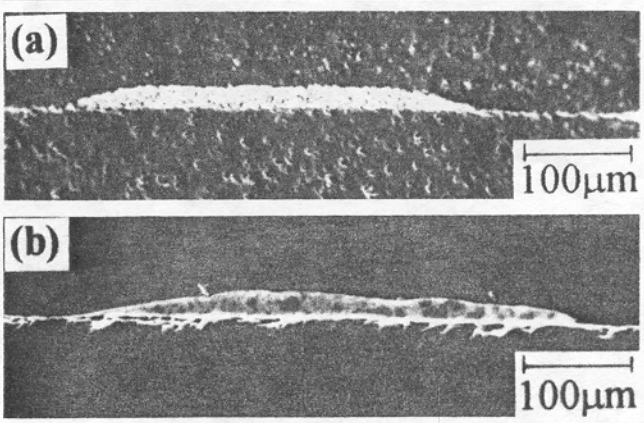

Fig. 13. Scanning electron microscopy photographs of the cross-sectional view after firing of (a) the A film, and (b) the B film. The bottom of each film is the Al_2O_3 substrate. The top of each film is the potting compound for mechanical polishing.

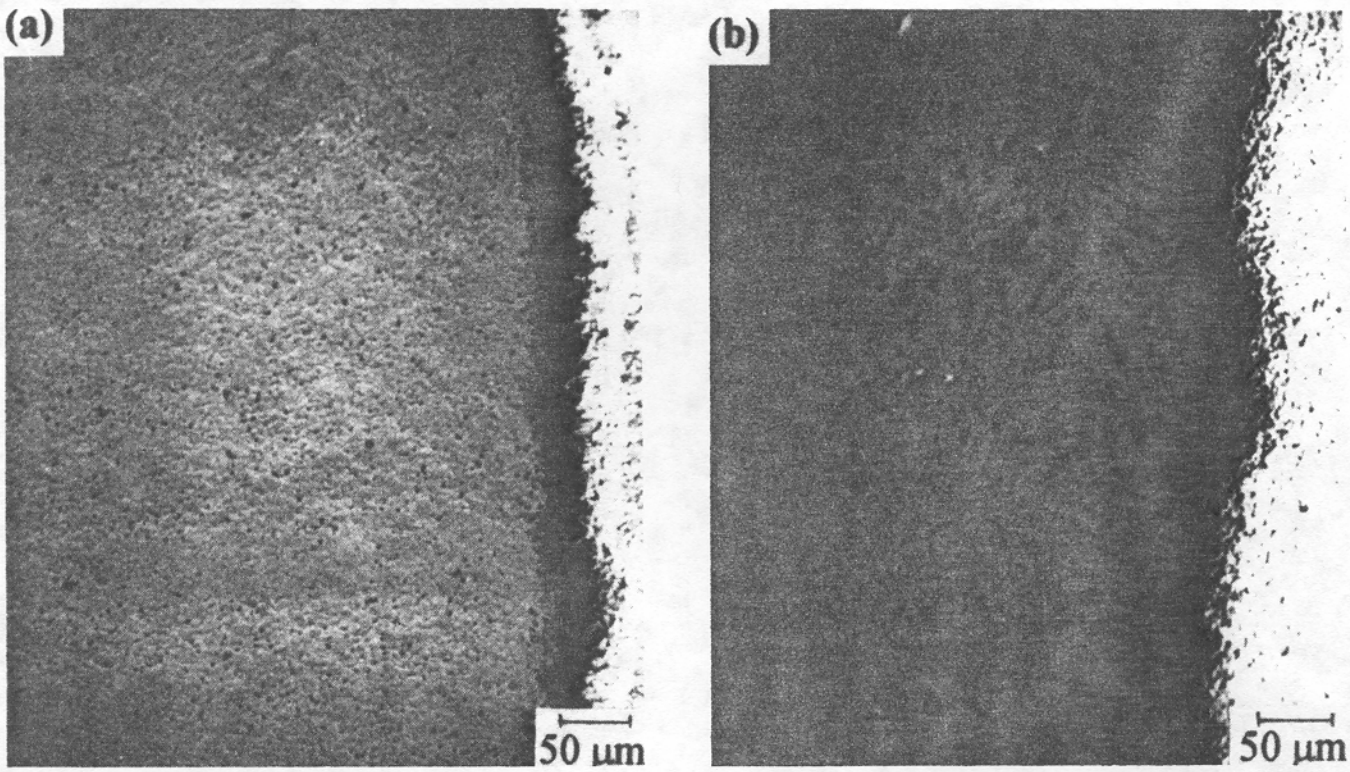

Fig. 14. Two SEM photographs of the top view of the edge of a printed conductor line after firing for (a) the A film, and (b) the B film.

Table V. Comparison Between the A Film and the B Film

	A	B
Electrical Resistivity (Ω.cm)	9.6×10^{-6}	2.3×10^{-6}
Solderability	Same for A and B	
Film/Al_2O_3 Adhesion		
Upon Peeling	2.0 ± 0.41 Kg	$>2.7 \pm 0.26$ Kg
Upon Pulling (tension)	8.8 ± 1.2 MPa	$>21.9 \pm 0.6$ MPa
Scratch Resistance	Better	Worse
Porosity	Large	Small
Pattern Definition		
Before Firing	Better	Worse
After Firing	Similar for A and B	
Average Particle Size in Paste (μm)	1	15–20
Firing Process	850°C in air	880°C in vacuum

strate bonding strength. In contrast, the A film had almost no reaction with the substrate. The weak bonding of the A film led to debonding at the film/substrate interface; this never occurred in the B-film case.

The 1–10 μm micropores of the A film shown in Fig. 4a and Fig. 6 are undesirable for the film's corrosion resistance. Since these micropores are good absorption sites, they may absorb much more moisture, cigarette smoke, and other contaminant atmosphere than the B film. Therefore, it is expected that the B film may have better corrosion resistance than the A film.

The two kinds of films were similar in solderability. This is because the B film had copper, which is less solderable than silver, while the A film had glass and porosity. The two kinds of films were also similar in the firing temperature, though firing needed to be performed in vacuum for the B film, while firing could be done in air for the A film. The vacuum requirement of firing the B film is a disadvantage.

The disadvantages of the B film compared to the A film are its lower scratch resistance (associated with the plasticity of a metal compared to a glass and the absence of glass in the B film) and poorer patternability before firing. The poor patternability of the B film before firing is largely due to the large particle size of the B paste, as shown in Fig. 11 and Fig. 12. Moreover, the vehicle used in the B paste was not designed for screen printing.

By adjusting the vehicle composition and using fine particles as well, the patternability of the B paste can be greatly improved. The disadvantage related to the low scratch resistance of the B film is not serious, since the interconnections are packaged. Another disadvantage of the B film is the high cost of the vacuum firing processing. However, it is possible to use an inert gas, such as Ar or N_2,[7] instead of vacuum during brazing in order to lower the processing cost of the B film. Hence, it is concluded that the active brazing alloy film (B film) is indeed viable for replacing the conventional Ag-glass thick film (A film) for interconnection applications.

CONCLUSION

A Ag-based Ti-containing brazing alloy, called an active brazing alloy, was found to be viable for serving as thick film interconnections in electronic packag-

ing. The paste containing the brazing alloy particles was applied to an alumina substrate by screen printing and subsequently fired at 880°C in vacuum. Compared to a conventional Ag-glass thick film, the brazing alloy film exhibited a lower volume electrical resistivity, much greater film/substrate adhesion, much lower porosity, similar solderability, lower scratch resistance, and poorer patternability before firing. The poorer patternability was due to the much larger particle size of the alloy paste compared to the Ag-glass paste, so this disadvantage could be removed by using brazing alloy particles of smaller size. The mechanism for film/substrate adhesion was associated with the reaction between the titanium in the brazing alloy and the substrate in the case of the brazing alloy film. In the case of the conventional Ag-glass film, the film/substrate adhesion was associated with the flow of the glass, which served as the binder.

ACKNOWLEDGMENT

This work was supported by the Advanced Research Projects Agency of the U.S. Department of Defense and the Center for Electronic and Electro-Optic Materials of the State University of New York at Buffalo.

REFERENCES

1. Rene E. Cote and Robert J. Bouchard, *Electronic Ceramics*, ed. Lionel M. Levinson, (New York: Marcel Dekker, Inc., 1988), Ch. 6, p. 307.
2. Howard Mizuhara and Toshi Ogama, *ASM Handbook*, Vol. 4 (Ceramics and Glasses).
3. W. Weise, W. Malikowski and W. Bohm, *Ceramic Ind.* 134 (2), 38 (1990).
4. *Method of Test for Wire Peel Adhesion of Soldered Thick Film Conductors to Ceramic Substrates*, DuPont Electronics.
5. *Standard Practice for Determining Solderability of Thick Film Conductors*, ASTM Designation: F357-78 (Reapproved 1991).
6. *Shear/Scratch Tester Manual*, Teledyne Taber Inc.
7. *Metz Brazing Products for Quality Metal Joining* Product Catalogue, Degussa.